Int. J. Heat Mass Transfer. Vol. 14, pp. 427–441. Pergamon Press 1971. Printed in Great Britain

SINGLE-PHASE TRANSPORT PROCESSES IN THE OPEN THERMOSYPHON

D. JAPIKSE* and E. R. F. WINTER†

Heat Transfer Laboratory, School of Mechanical Engineering, Purdue University, Lafayette, Indiana 47907, U.S.A.

(*Received* 4 *December* 1969 *and in revised form* 2 *June* 1970)

Abstract—A brief review of laminar flow and a new laminar boundary layer study showing good agreement with experimental data is given. The problem of determining transition from laminar to turbulent boundary layer flow is reviewed. The best available transition data are examined and it is argued that the velocity profile inflection point and the adverse pressure gradient in the core are causes of the trend obtained. The fully turbulent experimental results for $0{\cdot}005 < Pr < 200$ and $0{\cdot}6 < L/a < 100$ are found to follow a fixed relationship when the tube radius is used as a dimensional correlating parameter. Core-boundary layer entrainment, probably resulting from inlet conditions, seems to establish this dependence on radius.

NOMENCLATURE

a, tube radius, inside;
b_i, ordinate intercept values of certain linear correlations;
C_p, specific heat (at constant pressure);
d, tube diameter, inside;
g, gravitational acceleration;
h, convective heat transfer coefficient;
k, thermal conductivity;
L, tube length of the open thermosyphon or half-length of the closed thermosyphon;
$\dot{m}$, mass flow rate, non-dimensional $= \dot{M}C_p/kL$;
$\dot{M}$, mass flow rate, dimensional;
M_i, slope values of certain linear correlations;
p, pressure;
q, heat flux;
$\dot{Q}$, heat flow rate;
r, radius, non-dimensional $= R/a$;
R, radius, dimensional;
T, temperature, dimensional [°C];
ΔT, temperature difference;
u, velocity in x direction, non-dimensional $= a^2U/\alpha L$;
U, velocity in x direction, dimensional;
v, velocity in r direction, non-dimensional $= aV/\alpha$;
V, velocity in r direction, dimensional;
x, axial coordinate, non-dimensional measured from bottom $= X/L$;
X, axial coordinate, dimensional measured from bottom;
α, thermal diffusivity $= k/\rho C_p$;
β, coefficient of thermal expansion or the (complementary) thermal boundary layer thickness from tube centerline; depending on specific application;
γ, non-dimensional centerline velocity;
δ, momentum boundary layer thickness from tube centerline (complementary thickness);
θ, angle of inclination;
μ, viscosity, dynamic;
ν, viscosity, kinematic;
ρ, density.

* NDEA Fellow, presently Assistant Project Engineer, Turbine Group, 3S3, Pratt Whitney Aircraft, Division of United Aircraft Corp., 400 Main Street, East Hartford, Connecticut 06108.

† Professor of Mechanical Engineering.

Nondimensional groups

Gr, Grashof number $= \beta g \Delta T a^3/\nu^2$;
Pr, Prandtl number $= \mu C_p/k$;
Ra, Rayleigh number $= Gr\,Pr$;
Nu_a, Nusselt number (used for open system) $= ha/k = \dot{Q}/2\pi(T_1 - T_0)k$;
Nu_d, Nusselt number (used for closed system) $= hd/k = \dot{Q}/\pi(T_{1,1} - T_{1,2})k$;
t, $\beta g a^4 T/\nu\alpha L$;
t_{ot}, $\beta g a^4(T_1 - T_0)/\nu\alpha L$;
t_{ct}, $\beta g d^4(T_{1,1} - T_{1,2})/\nu\alpha L$.

Subscripts

a, based on radius;
b, condition at the base;
ct, closed thermosyphon;
mc, mixing cup (temperature);
ot, open thermosyphon;
1, condition at wall;
0, condition at orifice on the centerline;
1, 2, denotes bottom or top half respectively of closed thermosyphon; when paired subscripts are used the second number always denotes the tube half.

1. INTRODUCTION

THE THERMOSYPHON is a device which transfers heat, mass, and momentum by utilizing buoyancy forces on a fluid contained in a vessel. A net heat-transfer, effected at suitable points, is all that is required for continuous operation and mechanical inputs are excluded. Figure 1 shows certain specific types of thermosyphons which have received special attention. They are purely free convection devices, one being open and the other being closed. They may be single or two-phase, they may have any number of components and the body force field may be gravitational or centrifugal. It has become customary to call these two configurations simply open (Fig. 1a) and closed (Fig. 1b) thermosyphons.

Studies of the open system serve two fundamental purposes: (1) an understanding of the closed system (and other types of thermosyphons) is based on knowledge of the open system, as indeed this particular study is related to a companion study of the closed system, and (2) many phenomena observed in the open system are relevant to understanding other free convection internal flow processes. It will be seen that there are basic gaps in our knowledge of thermosyphon systems which can best be closed by a careful study of the open system. This study, therefore, concentrates on some of the outstanding problems of single

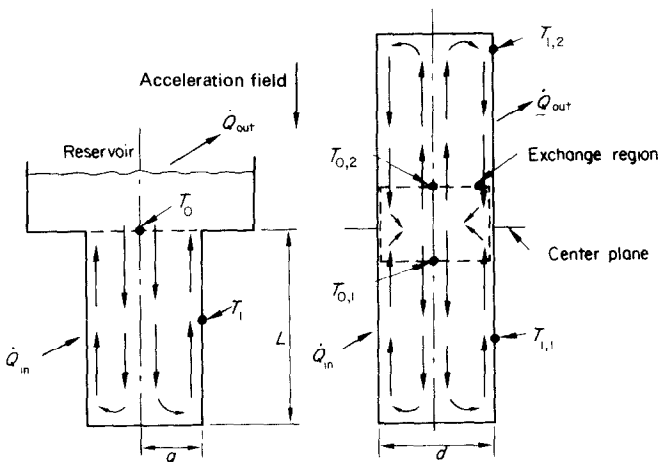

(a) Open thermosyphon (b) Closed thermosyphon

FIG. 1. Open and closed thermosyphons.

phase, single component open thermosyphon behavior.

Applications for these systems have been manifold but since the closed system has received greater industrial interest lately, a review of them is deferred to a subsequent publication [1]. Fundamentally, the open system is more attractive since it is generally capable of producing higher heat-transfer rates than the closed system and in some cases it should be possible to take advantage of them. For example, in the case of an emergency in a nuclear reactor it is necessary to expel large amounts of energy quickly. It might well be possible to cool the reactor with an open thermosyphon connected to a common industrial water supply located on the building roof which would form a natural reservoir for an open thermosyphon and would allow the discharge of a large amount of energy.

2. SUMMARY OF FUNDAMENTAL OPEN THERMOSYPHON BEHAVIOR

2.1 *Laminar flow*

As can be readily appreciated by studying Fig. 1a, the primary effect of heating the wall of an open thermosyphon should be to cause some type of flow upward along the wall due to buoyancy effects and an associated return flow downward in the core via continuity. Specifically, it has been found that for large heat fluxes the buoyancy forces are sufficiently intense near the wall so that a boundary layer regime is obtained. For weaker heat fluxes the buoyancy forces are less and the effect of shear is relatively enhanced causing the boundary layer to try to fill the entire tube or, in other words, for the effects of wall shear to be significant throughout the tube. Hence, compared with boundary layer flow, the flow is impeded. For sufficiently weak fluxes of thermal energy through the wall, this effect has been found to become rather uniform and a similarity flow is realized with, for still weaker fluxes, a stagnant bottom region. The effect of geometry, as expressed by L/a, is to accentuate the trend so that for increasing L/a larger values of Ra_a are necessary in order to attain any given heat flux level. The effect of property variations, as expressed by Pr, is to increase heat-transfer for increasing Pr under boundary layer conditions and to decrease it for the impeded or similarity flow conditions. Figure 2, in which mainly

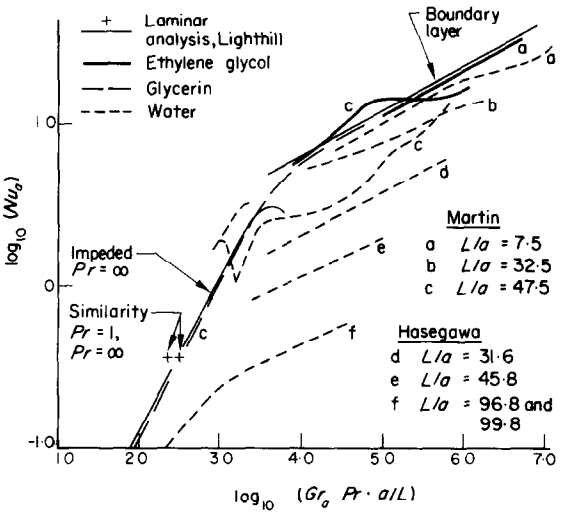

FIG. 2. Heat transfer in the open thermosyphon, $Pr > 1$.

experimental results from various workers for $Pr > 1$ are exhibited, shows these various regimes for laminar flow and various other results, presumably turbulent.

This brief description of the flow processes applies directly to laminar flow. It should be noted that Lighthill [2] analytically predicted quite accurately these three laminar flow regimes, for $Pr = \infty$ and $Pr = 1$, before any experimental results were available. Subsequently, Leslie and Martin [3] extended the similarity and boundary layer solutions to the case of arbitrary Pr, but still assuming equal momentum and thermal boundary layer thicknesses.

2.2 *Transition flow*

There are at least three factors which have been previously cited as contributors to the

generation of turbulence: (1) the cross-sectional distribution of shear has a maximum in the fluid, (2) the temperature gradient upwards can be negative, and (3) inlet turbulence may penetrate deeply. Naturally, viscous damping will tend to delay and to reduce the turbulent motion.

Martin [4] claimed that Lighthill's solution suggests

$$Re_{\text{crit.}} \propto \frac{Ra_a}{Pr} = Gr_a$$

so that a constant Gr_a should predict transition, when evaluated at the core conditions (constant T_0). Indeed, such critical Grashof values have been obtained for particular fluids in certain studies (note that this implies independence of L/a), but not in general.

2.3 *Turbulent flow*

The problem of describing turbulent flow processes in the open thermosyphon is at once far more complex than the laminar one. In fact, the various studies published to date are perhaps characterized better by their areas of disagreement rather than their areas of agreement.

A general picture can be obtained by noting (as did Lighthill [2]) that for laminar flow $\dot{Q} \propto \nu^{\frac{1}{4}}$ in the boundary layer regime and $\dot{Q} \propto \nu^{-1}$ in the impeded regime. Since turbulence is, in a gross sense, a large increase in ν (the other properties remaining fixed) one would anticipate a reduction of heat-transfer in the impeded regime under turbulent flow conditions and an increase in heat-transfer in the boundary layer regime. If, however, transition occurs in the first regime, this boundary layer regime might not be attainable and any subsequent increase might be only a general trend or tendency.

Figures 2 and 3 show experimental results which have been reported for turbulent flow for fluids with $Pr > 1$ and liquid metals, respectively. Referring first to the case where $Pr > 1$, the various workers have reported finding three types of turbulent flows: turbulent boundary layer with a laminar core, laminar boundary layer with a turbulent core and fully turbulent (impeded) flow. Hasegawa *et al.* [5] were able to correlate their experimental water results for fully turbulent flow but their correlation does not apply to Martin's [4] results. For liquid metals, it can be surmised that all three

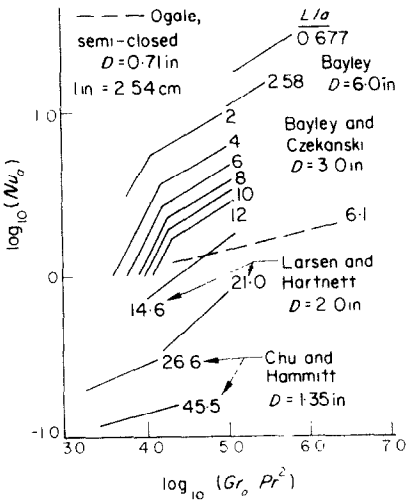

FIG. 3. Heat transfer in the open thermosyphon, liquid metals.

types again probably exist by considering the results of Bayley *et al.* [6, 7]. However, the empirical correlations from Bayley's studies do not agree with each other and neither predicts the results of other liquid metal studies.

Finally in spite of the numerous studies of open thermosyphon behavior, clearly several basic problems exist which are dealt with in the following sections: (1) a careful analytical study of laminar flow which gives the basis for defining necessary parameters which govern transition from laminar to turbulent flow and which results in several new parametric heat-transfer investigations, (2) a new examination of the causes of transition and (3) a new study of heat transfer under the turbulent-impeded conditions.

3. LAMINAR BOUNDARY LAYER HEAT TRANSFER

The analysis of this section concentrates on that laminar flow regime which provides the highest heat-transfer rates. The emphasis here will be on the physical process being modeled and the validity of the modeling assumptions. Therefore each detailed algebraic step, and there are many, is not given as they are carefully presented elsewhere [8]. Also certain similarities in the first part of the analysis to other treatments [2, 3, 9]* will be apparent and do not require detailed elaboration.

The basic equations are those for boundary layer flow since, as noted by Lighthill [2], the flow is either of the boundary layer type or L/a is large. This, however, is probably not true for liquid metals where all conduction terms can be significant. Also, for an isothermal base with small L/a with most any fluid the amount of heat transfer through the base can be very significant and the resulting process at the base may not give a boundary layer process in that region at the wall. Thus the following analysis is intended for an open thermosyphon with adiabatic base and Prandtl numbers greater than, say, 0·1. Thus,

$$\frac{\partial U}{\partial X} + \frac{\partial V}{\partial R} + \frac{V}{R} = 0 \tag{1}$$

$$U\frac{\partial T}{\partial X} + V\frac{\partial T}{\partial R} = \alpha\left(\frac{\partial^2 T}{\partial R^2} + \frac{1}{R}\frac{\partial T}{\partial R}\right) \tag{2}$$

$$U\frac{\partial U}{\partial X} + V\frac{\partial U}{\partial R} = -g - \frac{1}{\rho}\frac{\partial P}{\partial X} + \nu\left(\frac{\partial^2 U}{\partial R^2} + \frac{1}{R}\frac{\partial U}{\partial R}\right) \tag{3}$$

$$\frac{\partial P}{\partial R} = 0 \tag{4}$$

$$\rho^{-1} = \rho_1^{-1}\{1 + \beta(T - T_1)\} \tag{5}$$

and all properties, except ρ, are treated as constant. Lock [10] has shown that these properties should be modeled at the tube wall temperature. The boundary conditions are:

$$\text{at } R = a, \quad T = T_1(x) \quad \text{and} \quad U = V = 0$$
$$\text{at } X = 0, \quad \frac{\partial T}{\partial X} = 0 \quad \text{and} \quad U = V = 0 \tag{6}$$
$$\text{at } X = L \quad \text{and} \quad R = 0,\ T = T_0.$$

Following Lighthill rather closely, the pressure gradient term can be eliminated by applying the momentum equation at $R = a$ and the equations can be suitably non-dimensionalized* and integrated from $r = 0$ to 1 to give the following working set of equations:

Continuity:

$$\int_0^1 ru\,\mathrm{d}r = 0 \tag{7}$$

Energy:

$$\frac{\partial}{\partial x}\int_0^1 rut\,\mathrm{d}r = \left.\frac{\partial t}{\partial r}\right|_{r=1} \tag{8}$$

Momentum:

$$\int_0^1 (t - t_1)\,r\,\mathrm{d}r + \frac{1}{2}\left[\frac{\partial u}{\partial r} - \frac{\partial^2 u}{\partial r^2}\right]_{r=1} = \frac{1}{Pr}\frac{\partial}{\partial x}\int_0^1 ru^2\,\mathrm{d}r. \tag{9}$$

Also of value are the energy equation at $r = 1$,

$$\left[\frac{\partial^2 t}{\partial r^2} + \frac{\partial t}{\partial r}\right]_{r=1} = 0 \tag{10}$$

and the momentum equation at $r = 0$,

* Lighthill's study was for $Pr = \infty$ and $\beta = \delta$ whereas those of Leslie and Martin and Chu and Hammitt were for arbitrary Pr and $\beta = \delta$.

* For this study the temperature, T, and not the temperature difference, ΔT, has been non-dimensionalized simply to facilitate the parametric studies so that either part, but not all, of ΔT can be independently varied.

$$\left[\frac{1}{Pr}u\frac{\partial u}{\partial x}\right]_{r=0} = t_0 - t_1 + \left[\frac{\partial^2 u}{\partial r^2} + \frac{1}{r}\frac{\partial u}{\partial r}\right]_1^0 \quad (11)$$

where the non-dimensional boundary conditions are:

$$\text{at } r = 1, \quad t = t_1(x) \quad \text{and} \quad u = v = 0$$

$$x = 0, \quad \frac{\partial t}{\partial x} = 0 \quad \text{and} \quad u = v = 0 \quad (12)$$

$$x = 1 \text{ and } r = 0, t = t_0.$$

In previous analyses [2, 3] the term $\partial^2 u/\partial r^2$ was eliminated between equations (9) and (11) since Lighthill felt that any assumed profile would be rather insensitive to the true value of this term and hence a source of error. Consequently one less equation existed and only the case where $\beta = \delta$, or equal thermal and momentum boundary layer thicknesses, was treated. This, however, will not be followed here.

The earlier analyses also argued that the velocity and temperature profiles (which must be assumed when using the Karman–Pohlhausen method) should be even functions of radius and Lighthill cited (1) symmetry and (2) probable increased accuracy by assigning weight to different annuli based on their cross-sectional area, as reasons why even functions should be used. Now the "symmetry" argument, [$T(R) = T(-R)$ formally], as applied to radial variations, is considered to be a fallacy since negative radius is virtually meaningless in a cylinder.* Conservation principles might require a flat profile at the centerline but this is quite distinct and implies nothing about the evenness of the boundary layer profile. Concerning the second argument, it may be noted that no supporting evidence was given. Quite to the contrary, Bayley *et al.* [6] for liquid metals and this study using Foster's [11] data for water and oil found that cubic temperature profiles gave the best fit for the experimental data. The same was found for the closed thermosyphon [1].

* It is understood by the authors that the same fallacy exists in Heat Pipe literature.

Finally it may be noted that in the previous studies actually a cubic velocity profile and a parabolic temperature profile were used. The present investigation considers this case and also that with the cubic temperature profile.

Thus the following profiles were used:

$$t = a + br + cr^2 + dr^3 \qquad \beta \leqslant r \leqslant 1$$

$$t = t_0 \qquad 0 \leqslant r \leqslant \beta$$

$$u = \gamma(x)(a' + b'r + c'r^2 + d'r^3) \qquad \delta \leqslant r \leqslant 1$$

$$u = -\gamma(x) \qquad 0 \leqslant r \leqslant \delta$$

where the constants are evaluated using the boundary conditions and equations [7] and [10].

The choice of $u = -\gamma(x)$ in the core follows only from the boundary layer concept. Similarly $t = t_0$ in the core for this reason but now augmented by the fact that an adiabatic base is used.

These profiles allow the integration implied in equations (7)–(9) to be carried out so that ordinary differential equations of the following forms result:

$$\frac{\mathrm{d}}{\mathrm{d}x}F[\beta(x), \delta(x), \gamma(x), x] = f_1(x)/f_2[\beta(x)] \quad (13)$$

$$\frac{1}{Pr}\frac{\mathrm{d}}{\mathrm{d}x}G[\delta(x), \gamma(x), x] = g[\beta(x), \delta(x), \gamma(x), x] \quad (14)$$

$$\frac{\gamma}{Pr}\frac{\mathrm{d}\gamma}{\mathrm{d}x} + \gamma H[\delta(x), x] = h(x). \quad (15)$$

be performed and a system of three first order, non-linear, ordinary differential equations would result which could, in principle be solved by, say, Runge–Kutta integration for β, δ and γ. However, the functions F and G are already very lengthy and such differentiation would vastly increase the size of the system of equations and thus enhance the chance for round-off error, which was found to demand double-precision numerical calculations even with a simpler method. Thus the equations were partially

integrated as they are and the remaining integrals were replaced by summations which gave:

$$\beta_{n+1} = 6 - 2\sqrt{(4+\zeta)} - \beta_n;$$

$$\zeta = -\frac{6}{\Delta F_n}\int_{x_n}^{x_n+\Delta x_n}(t_0 - t_1)\,dx \tag{16}$$

$$G_{n+1} = G_n + Pr\,\Delta x_n \bar{g};$$

$$\bar{g} = g\left(x_n + \frac{\Delta x_n}{2}\right) \tag{17}$$

$$\gamma_{n+1} = \frac{h_{n+1}}{H_{n+1} + \dfrac{1}{Pr}\dfrac{\gamma_{n+1} - \gamma_n}{\Delta x_n}}. \tag{18}$$

Now these equations can be used in a forward stepping procedure but iteration at each step is clearly necessary to determine, and accurately, β_{n+1}, δ_{n+1} and γ_{n+1}. Knowing $\delta(1)$, $\beta(1)$ and $\gamma(1)$ the overall heat transfer rate follows from

$$Nu_a = \frac{F\{\beta(1), \delta(1), \gamma(1)\}}{t_1 - t_0}. \tag{19}$$

These calculations were carried out on a CDC 6500 computer. The technique performed quite well and showed good convergence as $\Delta x_n \to 0$. A solution, to 0·1 per cent accuracy for Nu_a, β and δ, required about 50 steps or about one to two minutes of computer time. The initial increment size, 0·002, was gradually increased as the boundary layer grew less rapidly. A given solution would typically include about 20000 iterative evaluations (total) but sometimes more. As stressed before, double precision computation was necessary.

Figure 4 presents a comparison of the results of this study, those of other workers and the experimental work of Martin [4]. The analytical results of Chu and Hammit [9] are omitted since they closely follow those of Leslie and Martin [3]. For fluids of large viscosity such as glycerin and rape seed oil (*Pr* effectively infinite) it can be seen that Lighthill's solution shows up to 7 per cent error whereas the others show up to 20 per cent error with the exception of this

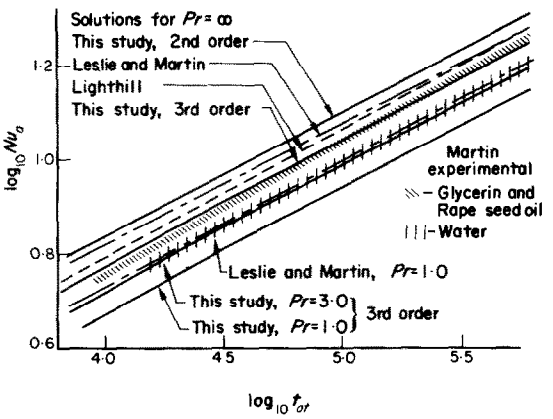

FIG. 4. Comparison of analytical and experimental results for heat transfer in the open thermosyphon with laminar boundary layer flow.

study using a third order temperature profile. Lighthill expected that his solution ($Pr = \infty$) would be good to within about 10 per cent at $Pr = 2$ but it is already high by about 17 per cent for the higher Prandtl numbers (between about 4 and 9) of water. Clearly the results of Leslie and Martin are too high at $Pr = 1$ and should fall well below the water data. The results of this study at $Pr = 3$ with a cubic temperature profile show reasonable agreement with the water data, though of course this curve is a little bit too high. The experimental data used for comparison are affected by the orifice shape, but only slightly [12]. In general it appears that a third order profile not only fits the temperature profile data well but also gives good heat transfer predictions. Also the necessity of using $\beta \neq \delta$ to model the boundary layer for variable Prandtl numbers is evident. Finally, a few results are also given in Fig. 5 which are useful for studies of closed thermosyphon behavior.

This study also was extended for $Pr < 1$ with solutions down to $Pr = 0{\cdot}025$ being obtained. Of interest was the fact that $\beta \simeq \delta$ at $Pr = 1{\cdot}0$. Hasegawa *et al.* [5] in an analytical free convection boundary layer analysis intended for an open thermosyphon study predicted that this

$$\log_{10}\ (Nu_a \cdot t_{at}) = M_1 \log_{10} t_{at} + b_1$$

$$\log_{10}\ (\dot{m}) = M_2 \log_{10} t_{at} + b_2$$

$$\log\ (t_{mc} - t_a) = M_3 \log_{10} t_{at} + b_3$$

$M_1 = 1{\cdot}26$, $M_2 = 0{\cdot}272$ and $M_3 = 0{\cdot}984$

Pr	b_1	b_2	b_3
∞	-0·243	0·172	-0·414
100	-0·246	0·161	-0·406
10	-0·265	0·0904	-0·354
3	-0·295	-0·00823	-0·285
1	-0·343	-0·137	-0·204

FIG. 5. Laminar open thermosyphon behavior.

should occur at $Pr = 0{\cdot}278$; but his conclusion is inconsistent with the concept that Pr represents the ratio of the momentum to the thermal transfer effects. Indeed a value of about unity is consistent with the results of classical convection studies. The heat-transfer results, however, for liquid metals did not show any sort of agreement with the results of Fig. 3, as indeed no other studies have. No doubt the omission of conduction effects is significant.

4. BOUNDARY LAYER TRANSITION BEHAVIOR

The problem of understanding the conditions under which transition in thermosyphons occurs has perplexed all workers in the thermosyphon field and is complicated by (1) seemingly unreliable thermosyphon transition data and (2) the inadequate state of present fundamental transition knowledge.

Part of the first problem is to separate data which really represent transition from laminar boundary layer flow (to turbulence) from that which may represent transition from an impeded flow. Both indeed form interesting problems but the attention here is restricted to boundary layer phenomena. Also, it is necessary to use accurate methods for detecting the transition.

For truly boundary layer processes, the following three methods, out of those which have been attempted, are considered to be reliable:

(1) Observing changes in radial (temperature) profiles from laminar to turbulent form (Bayley *et al.* [6]),

(2) Observing clear changes in the slope of Nu_a vs. t_{at} on a logarithmic plot (Martin [4] and others),

(3) Direct visual observation (Japikse [8]).

The first method is excellent in that it not only shows the occurrence of transition but it also clearly shows that laminar boundary layer flow did previously exist. The second method is reliable if it is clear that laminar boundary layer flow originally existed, and that such a sharp change in slope can only be caused by transition (not always true in the closed system). The third method is good if the visualization method clearly shows three-dimensional processes. It requires, however, some experience on the part of the experimenter to interpret various flow patterns. In contrast, the mere measurement of random temperature fluctuations at the wall or in the core is not adequate.

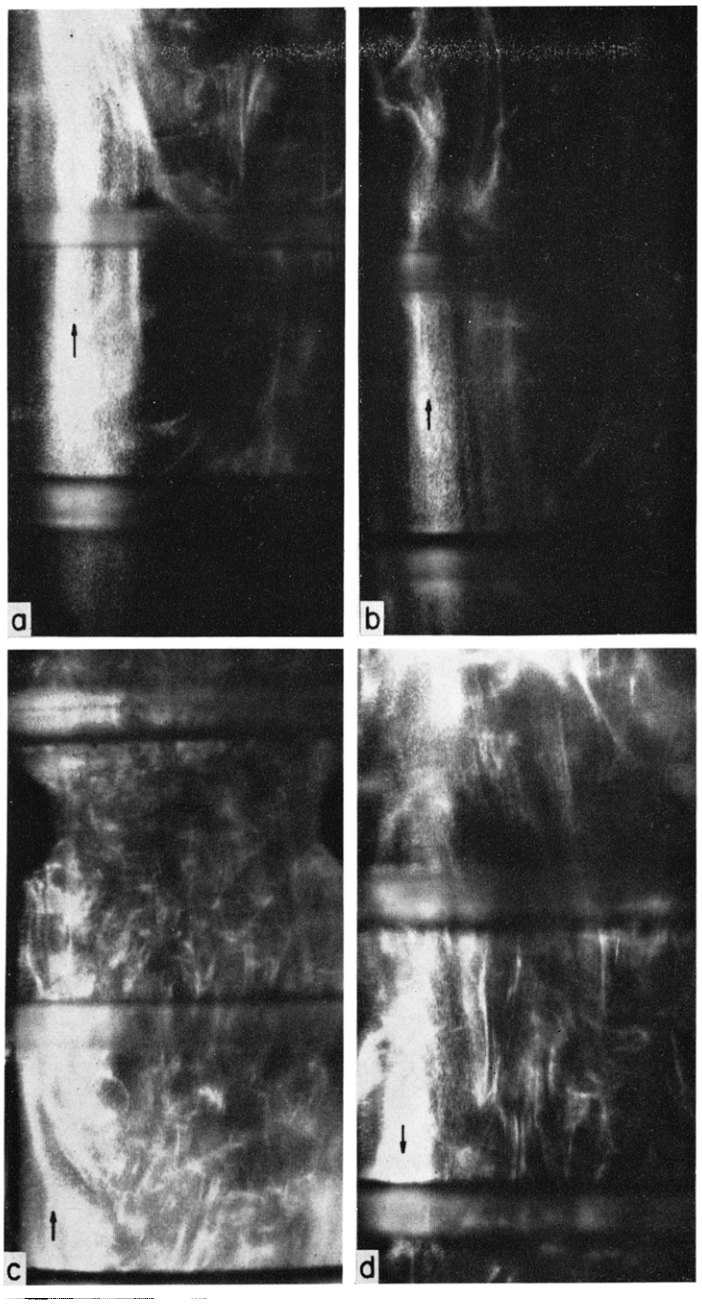

FIG. 6. Photographs showing the onset of turbulence in a closed thermosyphon. a—Laminar flow along the wall, bottom section; b—Laminar flow along the wall with transition to turbulence, bottom section; c—Turbulent core and boundary layer flow, bottom section; d—Flow approximately between "c" and "b" but in top section.

Notes: 1. The horizontal bands are flow dividers in the annulus only, i.e. exterior to the test section.

2. a, b and c are a complete sequence of photographs from the tube bottom to the mid-plane.

3. The flow visualization method utilizes "fish flakes" which both reflect and transmit light. a and b are primarily surface (i.e. $R=a$) flow effects whereas c and d include surface (where the arrows are) and internal effects.

[*facing page 434*]

Figure 6 shows some flow pictures (actually in a closed thermosyphon) using fish flakes in alcohol as a test fluid. Due to the tube curvature and the reflection/transmission characteristics of the fish flakes only a narrow band of flow is illuminated under laminar flow conditions. Picture (a), near the thermosyphon bottom, shows laminar boundary layer flow with occasional irregularities in the core which were caused at the mid-tube exchange region or, in an open thermosyphon, are known to be generated at the opening. Picture (b), about half way to the tube midplane, shows the beginning of transition while (c), near the mid-plane, shows fully turbulent flow. Picture (d), would fit roughly mid-way between (b) and (c) but in the top half of this closed thermosyphon. Now the important point is that even when laminar boundary layer flow exists at the wall (pictures a and b) it is possible to measure temperature variations in the core, due to irregularities carried down from the tube mid-section in the case of a closed thermosyphon or orifice for an open thermosyphon, or at the wall due to these irregularities being carried back up along the wall. Either case yielded random temperature measurements since the original generation of these irregularities is by no means regular. The flow itself, however, must be considered to be irregular but not turbulent. This point was further observed by using a tracer method which again showed the irregular twisting pattern but no dispersion normal to the instantaneous flow direction as would exist under turbulent flow conditions. By observing particular twisting elements of dye, it was noticed that through the core and into at least the first part of the boundary layer no evidence of amplification of the irregularities existed and hence some kind of stability was still present.

Similarly, the interpretation of wall heat flux measurements is quite risky since it presupposes a fundamental knowledge of the actual flow process. In general such knowledge is just not available and even current theories do not distinguish between turbulence and other irregularities (quasi-stable) which may, for example, come from the tube orifice. If, additionally, only boundary layer flow is known to exist, this method is reasonably safe.

Using the above three criteria the results of all thermosyphon workers were reviewed and three sets of data were found to meet all the above requirements. These include Bayley's [6] careful work for liquid metals; the closed

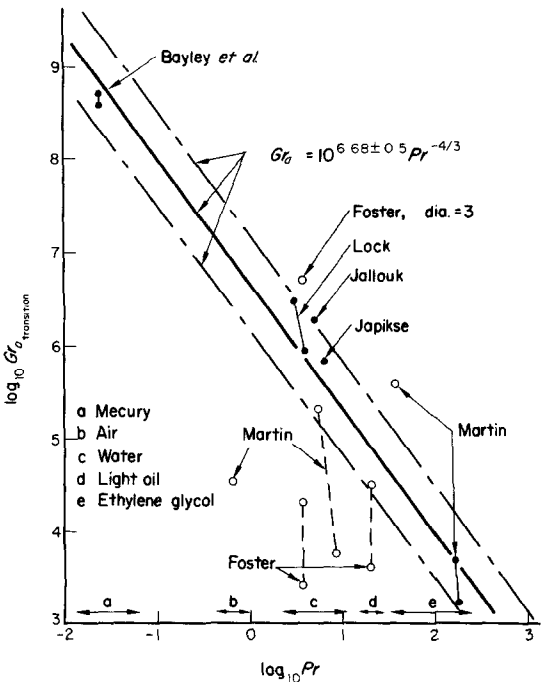

FIG. 7. *Gr* vs. *Pr* for transition to turbulence.

thermosyphon results* of Lock [10], Japikse [8] and Jallouk [13] (in which only boundary layer flow existed) for water; and Martin's [4] results for ethylene glycol. These values were determined based on methods one, two and three, and two respectively and are shown in Fig. 7 as solid dots. Also shown are the other reported transition values. Those for air and

* These results are divided by 2 since the temperature difference is approximately double; any consequent errors would be slight.

the lowest water value of Martin's are known to occur in impeded flow and most of the lower values from Martin and Foster with water and light oil probably are also.

These "pedigree" boundary layer results follow roughly the trend $Gr_{a_{crit}} = 10^{6.68 \pm 0.5} Pr^{-\frac{1}{4}}$ and show graphically the difficulty any worker would have in trying to obtain a constant value of Gr_a to characterize transition. Inasmuch as the variation band for each "pedigree" case in Fig. 7 is largely due to variations in L/a, the actual trend is of the form $Gr_{a_{crit}} = 10^{6.68 \pm 0.5} Pr^{-\frac{1}{4}} f(L/a)$ or $Ra_{a,crit.} = 10^{6.68 \pm 0.5} Pr^{-\frac{1}{4}} f(L/a)$. This relationship should be considered only as a formalism of the trend observed and not as a rigorous correlation due to the limited amount of reliable information. Clearly there is a need to reconsider first principles in order to explain this behaviour.

It was noted that Martin argued that Lighthill's laminar boundary layer analysis implied that a critical Reynolds number implies a critical Gr_a in the core region. This, however, simply is not correct and the actual results of that study show that Gr_a should increase with Pr in order to have a constant critical Reynolds number based on core conditions. The results of the previous section were also used to study how Gr_{crit} varies with Pr for a constant Reynolds number, based either on the core or maximum boundary layer velocity (or the sum of them) using either the tube radius or the maximum boundary layer thickness. In all cases Gr_a increased with Pr. Clearly this approach does not explain the observed phenomena.

The most probable explanation of the $Gr_{crit} \propto Pr^{-\frac{1}{4}}$ behaviour seems to be tied to the particular velocity and pressure distributions which occur in a thermosyphon, as both factors are known to be very important in determining a critical Reynolds number. In a thermosyphon, the pressure distribution is not constant and an inflection point exists in the velocity profile. Indeed, the occurrence of an inflection point in the velocity profile in an adverse pressure gradient can be highly conducive to transition (consider, for example, the classic stability analysis as in [14]).

In order to obtain a good theoretical basis for understanding this transition process, a stability analysis would be highly desirable but this would comprise a major study in itself. In order to assess the general effect of the particular pressure gradient and velocity profile, we can seek to answer the following question: given one known transition point on the Gr_a vs. Pr chart, under what restraint would it have to be bound if it were to trace out a transition curve? The answer appears to be, in a very simplified form, along a locus where t_{ot} is approximately constant. Under such a condition the pressure gradient was found, while studying the results of the last section, to scale on t_{ot} and show no significant further dependence on Pr. Similarly, the velocity profile depends most strongly on t_{ot} although there is some secondary dependence on Pr as well but this is a smaller effect. Thus since t_{ot} roughly fixes the profile, in which an inflection point occurs, as well as the pressure gradient which affects the magnification or attenuation of such instabilities, holding t_{ot} fixed should be approximately sufficient condition to trace out a plausible transition curve. If in reality such a transition curve is unique, then, within the limits of the approximations, this restraint should also be a necessary condition. Obviously t_{ot} = constant implies that $Gr_{crit} \propto Pr^{-1}(L/a)$.

This predicted trend is in qualitative agreement with what has been observed experimentally as far as the $Gr \propto Pr^{-1}$ is concerned. The experimental data are not clear concerning L/a effects (cases exist for both increasing and decreasing $Gr_{crit.}$ with L/a change) but there seems to be some tendency for $Gr_{crit.}$ to vary in an inverse manner, not directly, with L/a for boundary layer transition (this is more clearly so for transition from the impeded regime). Thus the form of $f(L/a)$, cannot be established at this time. Indeed, the above discussion is limited by the rather general approach taken and the fact that conventional stability studies were

used as a guide, which only give the start of instability, not actual transition. Nonetheless, the combination of profile instability and adverse pressure gradient in the thermosyphon core must be a significant cause of the trend found in Fig. 7.

5. THE IMPEDED TURBULENT REGIME*

This regime is by far the most significant mode of heat transfer to be found in the open thermosyphon from an application stand-point. It is not, however, well understood. Figures 2 and 3 show these data and at first it would appear that L/a is an extremely important correlating parameter, which it indeed is. However all known attempts, published and unpublished, fail to develop a complete correlation based on L/a which can predict all of the results. A careful review of the experiments showed that the Prandtl number and the diameter were changing between many experiments. The Prandtl number, however, was not always changing and the magnitude of the change when present was not sufficient to account for the changes in heat-transfer observed. The diameter, however, seemed to play a very important secondary role. Two cases exist in Fig. 2 and one in Fig. 3 where comparable L/a ratios have rather different heat transfer rates and the radii are indeed different.

The idea of introducing a dimensional variable into a heat transfer analysis is indeed strange. For the present, however, this lack of agreement with time-proven concepts of non-dimensional analysis will not be considered and a reconciliation will be sought later. The use of the radius or diameter as a correlating parameter is justified on the grounds of practicality and is motivated by the following experimentally based observations.

(1) The diameter appears as a meaningful parameter in heat transfer studies after L/d variations have already been considered (Figs. 2 and 3);
(2) This turbulent impeded flow regime, as it exists in the open thermosyphon, was not found in the closed thermosyphon under equivalent conditions but rather a boundary layer regime was found and the fundamental difference, the presence of an orifice, introduces only the diameter as a characteristic length [1];
(3) The diameter must play a singular role in characterizing effects such as inlet phenomena which can generate turbulence and a limit or constriction on the size of eddies which can be formed anywhere in the system.

The concept of mass entrainment, and hence thermal energy entrainment, is at once productive and must be applicable to the rather precarious balance between up flow and down flow found in the thermosyphon. Although the entrainment of cold core fluid into the boundary layer would, locally, enhance the overall heat-transfer rate the corresponding opposite effect of entraining heated boundary layer fluid into the core would reduce the driving potential $(T_1 - T_0)$ for all lower positions in the tube and this cumulative effect would easily offset the slight gain by the first process. Hence the case where radius effects are insignificant, i.e. $a \to \infty$, must be considered a limiting case. Thus, from classical studies,

$$Nu_a = C\,Ra_a^m, \qquad C = f(Pr) \tag{20}$$

would express the optimum heat-transfer under turbulent flow conditions. Judging from Figs. 2 and 3 and realizing the usual significance of a/L in thermosyphons, a more general relation must follow as

$$Nu_a = C_1\,Ra_a^m(a/L)^{C_2}, \quad C_1 = f(Pr) \tag{21}$$

* Whether this regime is actually turbulent or irregular laminar mixing or both cannot be completely determined at present. The name is used out of tradition and the comments of section 4 must be heeded.

where the data suggest that m should remain about the same throughout. If desired, of course, equation (21) can also be written in the more conventional form

$$Nu_a = B(Pr, a/L)t_{ot}^m$$

and

$$B(Pr, a/L) = C_1(Pr)(a/L)^{C_2 - m}.$$

Indeed various workers have found this form very suitable for their results although it failed when applied to other studies with different tubes. Now the degrading effect of entrainment must be confined to the term $C_1(a/L)^{C_2}$ and thus both C_1 and C_2 can be postulated to be functions of radius. Although C_2 might be a function of Pr as well, the fact that it is associated with a purely geometrical term might suggest an independence of Pr. Equations (20) and (21) imply that as $a \to \infty$, $C_2 \to 0$ but of course C_1 cannot. Now the latter part of item (3) above also implies that as $a \to 0$, C_1 and $C_2 \to$ const. since there should be a point where the smallness of the tube diameter will always restrict the eddy size possible for entrainment and any further increase in entrainment rate is blocked as the radius is decreased. Thus C_1 must be constant for small radii and also as $a \to \infty$ but may be a function of radius in between and C_2 must be a constant for small radii and approach zero as $a \to \infty$.

After studying the three points raised above and this predicted behavior that one might expect based on entrainment theory, an effort was made to piece together the results of all workers (with the isothermal wall conditions) into the form of equation (21). These are shown in Fig. 8 and the results are encouraging. Not only are the predicted trends obtained satisfactorily and, apparently, rather uniquely, but also the parameter C_2 appears to be a function only of radius. The choice of $m = 0{\cdot}25$ for water and $m = 0{\cdot}3$ for mercury was only used so as to be consistent with what has been used by most authors for those fluids. The data from Larsen and Hartnett [15] give the only real

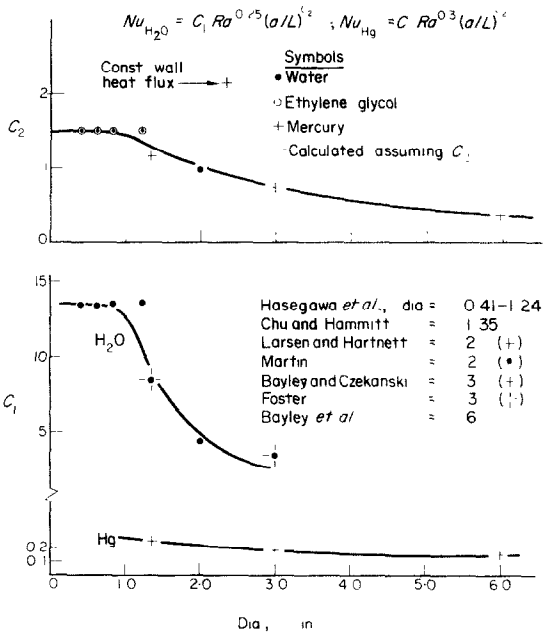

FIG. 8. Heat transfer correlations for turbulent impeded flow in the open thermosyphon, dia. in in.; 1 in. = 2·54 cm

exception to the trends observed and it can only be concluded that the method they used to average the wall temperature distribution for their case of constant heat flux is only adequate to represent the gross characteristics as shown in Fig. 3. A word of caution must also be interjected because the data for the first four and last two points on the C_2 graph were taken directly from the original correlations. While this is convenient and avoids errors due to recomputation, the presence of terms such as 3/2 for C_2, for example, indicates that the value might have been slightly idealized in the original study and might give a small shift from what is shown in these figures. The point shown for Martin ($D = 2$ in.) was calculated from his data where the strongest reduction in heat-transfer occurred for all L/a cases, i.e. $Ra = 10^{6 \cdot 5}$. At $Ra = 10^{7 \cdot 5}$, however, C_2 dropped to a lower value of 0·44 as can be expected from Fig. 2.

This exception found in Martin's data may be of extreme importance. Although the behaviour

expressed by equation (21) with C_1 and C_2 as function of radius is undoubtedly caused by entrainment, nothing has yet been said about the initial cause or source of the eddying motion which is responsible for this process. Indeed, this process generally begins before normal boundary layer transition would be expected (see Fig. 7) and, too, it is possible to obtain a purely turbulent boundary layer flow without the degrading entrainment effect (e.g. ethylene glycol, Fig. 2). As indicated in items (2) and (3) concerning diameter effects, the inlet effects may be of considerable importance. Indeed, it appears that Martin's studies were with a rounded inlet lip whereas the others were apparently with a sharp lip.

Martin and Lockwood [12] have also studied the influence of inlet orifice shape on flow patterns and heat-transfer rates. Unfortunately, the tests were carried out only for $L/a = 15$ which is a rather weak test and, further, the diameter of the transparent test apparatus was half the diameter of the corresponding heat-transfer apparatus. Some influence of the shape was found, though, on both the slope and magnitude of the heat transfer results with turbulent flow. The results with the sharp edged orifice were a bit more consistent with those of other investigators (with respect to the slope of the heat-transfer results in particular) than the rounded edge orifice results. However, in spite of this effect being evident, no significant impedence, as evidenced in heat transfer rates, was obtained in their study and clearly a more detailed investigation is necessary for an adequate understanding.

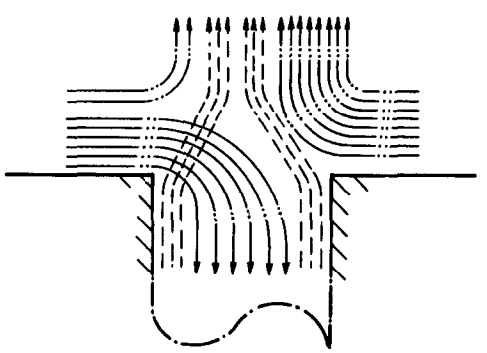

FIG. 9. Open thermosyphon inlet flow pattern, after [12].

Figure 9 shows a flow pattern observed by Martin and Lockwood which was unsteady in nature. For higher heat fluxes the pattern degenerated to extensive mixing. As the heat transfer rate increased, this inlet mixing was observed to penetrate further and further into the tube core. Thus a possible source, characterized by the diameter, is present for the turbulent impeded phenomena. It might well be possible, by using a flow guide at the orifice, to avoid or reduce the impeding effect, by forcing the boundary layer flow out along the reservoir floor and drawing the core flow from the center. For liquid metals this involves two orders of magnitude on heat-transfer rates. Other reservoir conditions, such as the size and location of the cooling coil, may also affect the nature of the inlet turbulence.

Now the question of the appropriateness of using a dimensional parameter can be reconsidered. It is felt that the same good agreement found with equation (21) would probably also be obtained if the system to which non-dimensional reasoning was applied were enlarged to include the entire orifice region, including at least part of the reservoir, and additional variables of which all have probably not yet been discovered. The radius of the orifice lip might be one such addition variable. Other variables might include reservoir and cooling coil dimensions. It is certainly true that the use of the unconventional dimensional parameter is fundamentally disturbing and thus further investigation into this phenomenon would be highly desirable. For the present, however, Fig. 8 shows that satisfactory results can be uniformly obtained from equation (21) with the use of a dimensional parameter, provided this equation is applied to systems not too different from those for which the experiments were made, particularly in regard to the nature of the reservoir and the inlet.

6. SUMMARY

An analytical study of laminar boundary layer heat-transfer in the open thermosyphon has been given which shows good agreement with experimental data.

The problem of determining boundary layer transitions was found to require careful evaluation of experimental data. The best data follows the trend $Gr_{crit} = 10^C Pr^{-\frac{4}{3}}$ were $C = 6{\cdot}68 \pm 0{\cdot}5$ and it is believed that the instability caused by the velocity profile inflection between the up flow and the down flow augmented by the adverse pressure gradient is a major contributor to transition.

The important turbulent-impeded regime was found to give heat transfer rates which follow the equation

$$Nu_a = C_1 Ra_a^m (a/L)^{C_2}$$

where C_1 and C_2 are functions of tube radius and C_1 depends on the Prandtl number as well. Entrainment, which causes the process described by this equation, may be originated by inlet orifice conditions. The possibility therefore exists for improved heat transfer rates if a flow guide is used at the orifice.

ACKNOWLEDGEMENTS

One of the authors (D.J.) wishes to acknowledge the support under an NDEA Title IV Fellowship which made this work possible and a subsequent NSF Post-Doctoral Fellowship under which some of the work on turbulent conditions was done.

REFERENCES

1. D. JAPIKSE, P. A. JALLOUK and E. R. F. WINTER, Single-phase transport processes in the closed thermosyphon, *Int. J. Heat Mass Transfer* (to be published).
2. M. J. LIGHTHILL, Theoretical considerations on free convection in tubes, *Q. J. Mech. Appl. Math.* **4** (pt 4), 398–439 (1953).
3. F. M. LESLIE and B. W. MARTIN, Laminar flow in the open thermosyphon with special reference to small Prandtl numbers, *J. Mech. Engng Sci.* **1**(2), 184–93 (1959).
4. B. W. MARTIN, Free convection in an open thermosyphon with special reference to turbulent flow, *Proc. R. Soc.* **230** (Ser A), 502–530 (1955).
5. S. HASEGAWA, K. NISHIKAWA and K. YAMAGATA, Heat transfer in an open thermosyphon, *Bull. Jap. Soc. Mech. Engrs* **6** (22), 230–50 (1963).
6. F. J. BAYLEY, P. A. MILNE and D. E. STODDART, Heat transfer by free convection in a liquid metal, *Proc. R. Soc.* **265** (Ser A), 97–108 (1961).
7. F. J. BAYLEY and J. CZEKANSKI, Experimental investigation of free convection in a liquid in long tubes, *J. Mech. Engng Sci.* **5**(7), 295–302 (1963).
8. D. JAPIKSE, Heat transfer in open and closed thermosyphons, Ph.D. Thesis, Purdue University, January (1969).
9. P. T. CHU and F. G. HAMMITT, Natural convection inside a circular cavity, ASME Paper 65-WA/HT-51 15 p. (1964).
10. G. S. H. LOCK, Heat transfer studies of the closed thermosyphon, Ph.D. Thesis, University of Durham (England), June (1962).
11. C. V. FOSTER, Heat transfer by free convection to fluids contained in vertical tubes, Ph.D. Dissertation, University of Delaware, June (1953).
12. B. W. MARTIN and F. C. LOCKWOOD, Entry effects in the open thermosyphon, *J. Fluid Mech.* **19** (pt 2), 246–56 (1963).
13. P. A. JALLOUK, Experimental investigation of heat transfer in a closed thermosyphon, M.Sc. Thesis, Purdue University (June 1969).
14. H. SCHLICHTING, *Boundary Layer Theory*, 4th edn., p. 409. McGraw-Hill, New York (1962).
15. F. W. LARSEN and J. P. HARTNETT, Effect of aspect ratio and tube orientation on free convection heat transfer to water and mercury in enclosed circular tubes, *J. Heat Transfer* **83**, 87–93 (1961).

Note: References [8] and [13] can be obtained from University Microfilm, Inc., Ann Arbor Michigan; U.S.A.

PROCESSUS DE TRANSPORT MONOPHASIQUE DANS UN THERMOSYPHON OUVERT

Résumé—On donne une revue brève sur l'écoulement laminaire et une nouvelle étude de couche limite laminaire montrant un bon accord avec les résultats expérimentaux. On étudie la détermination de la transition entre laminaire et turbulent pour un écoulement à couche limite. On examine les meilleurs résultats utilisables pour la transition et on montre que le point d'inflexion du profil des vitesses et le gradient adverse de pression dans le coeur du fluide sont les causes de la situation observée. On remarque que tous les résultats expérimentaux relatifs au régime pleinement turbulent pour $0{,}005 < Pr < 200$ et $0{,}6 < L/a < 100$ suivent une même loi quand le diamètre du tube est utilisé comme paramètre de corrélation dimensionnel. L'entrainement du coeur du fluide par la couche limite résultant probablement des conditions d'entrée, semble établir cette dépendance au rayon.

EINPHASIGE TRANSPORTVORGÄNGE IM OFFENEN THERMOSYPHON

Zusammenfassung—Es wird ein kurzer Überblick über die laminare Strömung gegeben und eine neue Studie über laminare Grenzschicht, die gute Übereinstimmung mit experimentellen Daten zeigt. Das Problem, den Übergang von laminarer zu turbulenter Grenzschichtströmung zu bestimmen, wird untersucht. Die vorhandenen Bestwerte für den Übergang werden geprüft, und es wird behauptet, dass der Wendepunkt des Geschwindigkeitsprofils und der entgegengesetzte Druckgradient im Strömungskern Gründe für die vorliegende Tendenz sind. Es zeigt sich, dass die Versuchsergebnisse bei vollturbulenter Strömung für $0{,}005 < \mathrm{Pr} < 200$ und $0{,}6 < L/a < 100$ einer festen Beziehung folgen, wenn der Rohrradius als dimensionsbehafteter Parameter benützt wird. Das Mitreissen des Strömungskerns durch die Grenzschicht, das wahrscheinlich durch die Einlaufbedingungen verursacht wird, scheint diese Abhängigkeit vom Radius zu bestärken.

ОДНОФАЗНЫЕ ПРОЦЕССЫ ПЕРЕНОСА В ОТКРЫТОМ ТЕРМОСИФОНЕ

Аннотация—Приводится краткий обзор работ по ламинарному движению; получены новые результаты по ламинарному пограничному слою, которые хорошо согласуются с экспериментальными данными. Рассматривается задача по определению условий перехода от ламинарного режима течения в пограничном слое к турбулентному. Обсуждаются наиболее надежные данные по переходному режиму и показывается, что точка перегиба профиля скоростей и положительный градиент давления в ядре потока определяют характер режима движения. Найдено, что по развитому турбулентному течению экспериментальные данные при $0{,}005 < Pr < 200$ и $0{,}6 < L/a < 100$ подчиняются установленной зависимости для случая, когда радиус трубы используется в качестве параметра корреляции. Вероятно отрыв пограничного слоя в ядре, зависящий от условий на входе, предопределяет эту зависимость от радиуса.